AN ANALYSIS OF RSS THRESHOLD OPTIMISATION USING FILTERING TECHNIQUES

[#1]**BOORLA SANTHOSH,** Research Scholar,
[#2]**Dr. T.SRINIVAS,** Professor & Co-Guide,
DEPARTMENT OF ELECTRONICS AND COMMUNICATION ENGINEERING,
SHRI JAGDISH PRASAD JHABARMAL TIBREWALA UNIVERSITY, RAJASTHAN.

ABSTRACT: There is a big trend nowadays to use event-triggered proximity report for indoor positioning. This paper presents a generic received-signal-strength (RSS) threshold optimization framework for generating informative proximity reports. The proposed framework contains five main building blocks, namely the deployment information, RSS model, positioning metric selection, optimization process and management. Among others, we focus on Gaussian process regression (GPR) based RSS models and positioning metric computation. The optimal RSS threshold is found through minimizing the best achievable localization root-mean-square-error formulated with the aid of fundamental lower bound analysis. Computational complexity is compared for different RSS models and different fundamental lower bounds. The resulting optimal RSS threshold enables enhanced performance of new fashioned low-cost and low-complex proximity report based positioning algorithms. The proposed framework is validated with real measurements collected in an office area where bluetooth-low-energy (BLE) beacons are deployed.

Index Terms—*Gaussian process, indoor positioning, proximity report, received-signal-strength, threshold optimization.*

1. INTRODUCTION

Over the past few years, indoor localization and tracking using wireless networks has received considerable attention due to the ever increasing demand on location-awareness in various sectors. So far, most of the efforts have been made to improve the localization accuracy using advanced technologies, for instance statistical sensor fusion, dedicated to optimally fuse different types of position-related measurements collected from indoor wireless infrastructures (for instance, cellular, wireless fidelity (Wi-Fi) and bluetooth low-energy (BLE) nodes and mobile devices. Due to the rapid development of the beaconing techniques, there is a big trend nowadays to use event-triggered proximity information for developing new-fashioned, low-cost (e.g., less communication overhead, smaller database for storage, cheaper deployment and maintenance) indoor positioning systems.

One way of obtaining a proximity report from the network is to compare an instantaneous RSS value with a tuned threshold Pth. A proximity report obtained in such way indicates whether or not a user equipment (UE) is in proximity of a reference network node. Essentially, a proximity measurement can be treated as a quantized RSS with merely two quantization levels. Unlike in the conventional paradigm, where the UE sends the measured RSS indication values periodically to the core network, a proximity report is triggered only when the UE's status changes, for instance when the UE is crossing a border to another service region. Such proximity reporting scheme is beneficial in various ways. Among other benefits, the signaling between the UE and the core network can be significantly reduced by sending much less frequently 1-bit proximity values instead of 6-8 bits RSS indication values proximity values instead of 6-8 bits RSS indication values.

In order to explain the concept of proximity based noncooperative indoor positioning more clearly, we give an illustrative example in Fig, wherein we assume noise free RSS measurements and a simplistic propagation model with which an RSS threshold corresponds to a circular coverage area in open space. As we can see from the figure, the service area is divided into several small regions. An instantaneous RSS measurement being larger than a predefined threshold implies that the UE resides in the corresponding coverage area. For instance, the proximity vector, e.g., [1, 1, 0], indicates that the UE is in the coverage area of the first and the second reference nodes, while outside of the coverage area of the third reference node. The UE needs to upload the proximity vector only if there is status change in the proximity report, for instance from [1, 1, 0] to [0, 1, 0], when the UE moved from the marked place some distance to the right. However, we note that in practice the RSS measurements are subject to various types of noise and we resort to a statistical framework for RSS thresholding.

 Copyright @ 2022 Author

ISSN: 2278-4632
Vol-12 Issue-01 No.01: 2022

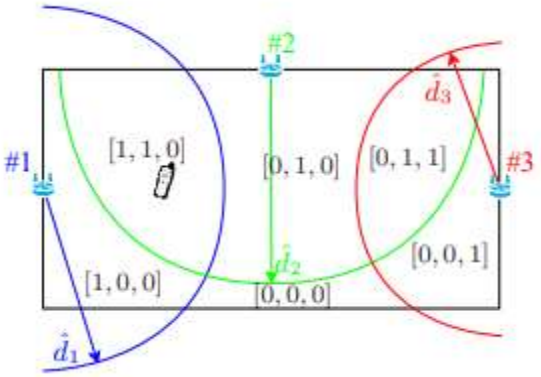

Fig.. Illustration of proximity report based indoor positioning. In this example, three reference nodes are deployed in a service area for positioning purposes. For simplicity, we assume that the RSS measurements are noise free and the underlying propagation model fits a linear log-distance model, cf. Section II-B. The coverage radius of each node, dˆ i, i = 1, 2, 3, is simply determined by dˆ i = d0 · 10 Pth,i−Aˆ i 10Bˆ i , where the notations will be explained later on. As we can see, the service area is divided into several small regions. An instantaneous RSS measurement being larger than a predefined threshold implies that the UE resides in the corresponding coverage area. For instance, the proximity vector, e.g., [1, 1, 0], indicates that the UE is in the coverage area of the first and the second reference nodes, while outside of the coverage area of the third reference node. The UE needs to upload the proximity vector if and only if there is at least one entry reversing the status, for instance from [1, 1, 0] to [0, 1, 0], when the UE moved from the marked place some distance to the right.

2. RELATED WORK

In the literature, the proximity based positioning algorithms are often called coarse grained algorithms or range-free algorithms. Since the publication of a plethora of proximity based positioning algorithms have been proposed, including the centroid algorithm, the approximate point in triangle (APIT) algorithm, the maximum-likelihood estimation based algorithm, the ecolocation algorithm and the iterative learning based algorithm, to mention a few. The majority of the existing work considered large-scale cooperative sensor network localization subject to communication constraints. To the best of our knowledge, RSS thresholding was first considered for cooperative localization. Therein, a single RSS threshold is optimized so as to limit the number of the neighboring senors. In our recent work, RSS thresholding was considered for non-cooperative, infrastructure-based indoor positioning, which can be regarded as a special case. But the focus of lies in the overall positioning performance in a given service area and thorough treatment on the measurement campaign, RSS modeling, model fitting and parameter calibration, signaling, and performance evaluation using real data measured from a live network. In this work, we extend to multiple RSS thresholds tuning. The performance metric to be optimized is selected to be the overall positioning root-mean-square-error (RMSE) represented in terms of the Cram´er-Rao bound or Barankin bound. The former bound is suitable to benchmark estimation performance for mediumand large scale sensor networks, while the latter bound is more suitable to benchmark small scale sensor networks. Moreover, we introduce advanced Gaussian process regression (GPR) based RSS models, perform detailed performance analyses and validate the results with more real data. Lastly, we incorporate the derived fundamental lower bounds and the advanced GPR based RSS models into RSS thresholds optimization. To give a quick overview, the proposed generic framework for selecting a set of reasonable RSS thresholds for proximity report based positioning is given in Figure.

Copyright @ 2022 Author

ISSN: 2278-4632
Vol-12 Issue-01 No.01: 2022

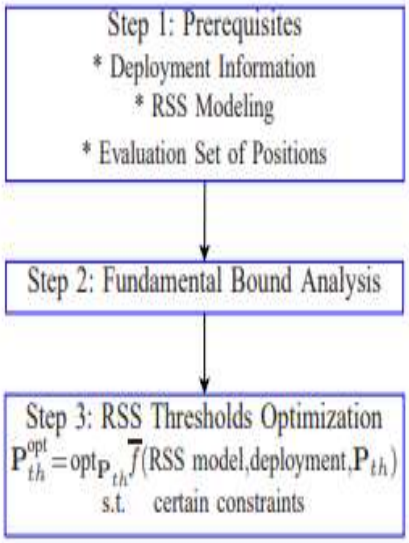

Fig. Key steps of the proposed RSS thresholds optimization procedure. Herein, P opt th represents the optimized RSS thresholds. The connections are the following. The fundamental bound analysis is based on deployment information and RSS modeling. The outcome of the fundamental bound analysis is the best achievable RMSE expression. Together with the evaluation set of positions, they are combined to evaluate the overall best achievable positioning accuracy as a function of the rss threshold.

3. SYSTEM ANALYSIS

RSS THRESHOLD OPTIMIZATION

In this section, we first define an optimization problem based on our objective, and then, we come up with an objective function that satisfies the optimization problem statement. Then, we propose a suitable optimization method and a multi-sensor sampling method (which provides RSS gradient inputs to the optimization algorithm). Then, we present a position controller that implements the optimization algorithm. The algorithm itself is summarized at the end of this section.

OPTIMIZATION PROBLEM

Let the measured RSS at the relay node from the client node be $RSS_c = RSS_c^{fs}(\|p_r - p_c\|) + \Phi_c^{sh}(p_r, p_c) + \Omega_c^{mp}(p_r, p_c, t)$ and from the server node be $RSS_s = RSS_s^{fs}(\|p_r - p_s\|) + \Phi_s^{sh}(p_r, p_s) + \Omega_s^{mp}(p_r, p_s, t)$ A way to solve Problem 1 is to find a function that maximizes both the RSSc and RSSs at the same time, so that the total good put is at a maximum. Figure shows the RSS readings as the relay node travels between the server and client nodes. The reason for non-symmetrical RSS values between the two nodes is that the environment has NLOS conditions and, hence, has different propagation constants. It can be observed from this figure that the good put is maximal when RSSs and RSSc become close to each other, and this is the basis for the objective of this work, i.e., to maximize the network capacity by maintaining a balance between radio signal strengths received from the server and the client nodes while attempting to maximize the RSS from both sides at the same time. It is also worth noting that this figure shows a one-dimensional RSS measurement, and if extrapolated to a 2D scenario, there can be multiple possible positions where RSSc and RSSs are equal, as will be shown later. Hence, it is important to consider a function that maximizes the values of RSSc and RSSs together while maintaining them as close as possible. The objective of the optimization problem can be formulated as follows:

$$p_r^* = \arg\max_{p_r} f(p_r);\ \text{s.t. } G(p_r^*) = \max_{p_r} G(p_r) \text{ and } RSS_c(p_r^*) = RSS_s(p_r^*);\ \forall p_r \in [p_s, p_c]$$

where G(pr) is the goodput value when the relay node is at position pr. The position of the relay node pr = (xr ∈ R, yr ∈ R) (whose value ranges between the positions of server and client nodes) is the control variable (argument), and the function f(pr) : R n → R is the objective function to be maximized in the optimization

Copyright @ 2022 Author

ISSN: 2278-4632
Vol-12 Issue-01 No.01: 2022

problem. $p * r$ is the position at which the objective function f(pr) is maximum and also the following two constraints are achieved: maximum goodput; RSSc and RSSs values match each other.

Algorithm 1 Robust stochastic optimization algorithm for RSS balancing between two wireless nodes.

Inputs: $x^i, y^i, \Delta x, \Delta y, \kappa, RSS_{\text{threshold}}, RSS_{\text{difference}}, g_{\text{threshold}}$
Outputs: x^{i+1}, y^{i+1}
if $(\overline{RSS_s} < RSS_{\text{threshold}}$ or $\overline{RSS_c} < RSS_{\text{threshold}})$ **then**
  while $(|\overline{RSS_s} - \overline{RSS_c}| \not\leq RSS_{\text{difference}})$ and $(\|g\| \not\leq g_{\text{threshold}})$ **do**
    Multi-sensor spatial sampling and filtering ()
      $\overrightarrow{RSS_c} = [RSS_c(x^i \pm \Delta x), RSS_c(y^i \pm \Delta y), \overline{RSS_c}(x^i, y^i)]$
      $\overrightarrow{RSS_s} = [RSS_s(x^i \pm \Delta x), RSS_s(y^i \pm \Delta y), \overline{RSS_s}(x^i, y^i)]$
      $[\overrightarrow{RSS_c}, \overrightarrow{RSS_s}] =$ Spatial Filtering$(\overrightarrow{RSS_c}, \overrightarrow{RSS_s})$
      $[\overrightarrow{RSS_c}, \overrightarrow{RSS_s}] =$ Temporal Filtering$(\overrightarrow{RSS_c}, \overrightarrow{RSS_s})$
    RSS Gradient Estimation ()
      $\nabla_x RSS_c = \frac{RSS_c(x+\Delta x) - RSS_c(x-\Delta x)}{2\Delta x}, \nabla_y RSS_c = \frac{RSS_c(y+\Delta y) - RSS_c(y-\Delta y)}{2\Delta y}$
      $\nabla_x RSS_s = \frac{RSS_s(x+\Delta x) - \overline{RSS_s}(x-\Delta x)}{2\Delta x}, \nabla_y RSS_s = \frac{\overline{RSS_s}(y+\Delta y) - \overline{RSS_s}(y-\Delta y)}{2\Delta y}$
    Gradient Normalization ()
      $\nabla RSS_c = \sqrt{\nabla_x RSS_c^2 + \nabla_x RSS_c^2}, \nabla RSS_s = \sqrt{\nabla_x RSS_s^2 + \nabla_x RSS_s^2}$
      $\|\nabla_x RSS_c\| = \frac{\nabla_x RSS_c}{\nabla RSS_c}, \|\nabla_y RSS_c\| = \frac{\nabla_y RSS_c}{\nabla RSS_c}$
      $\|\nabla_x RSS_s\| = \frac{\nabla_x RSS_s}{\nabla RSS_s}, \|\nabla_y RSS_s\| = \frac{\nabla_y RSS_s}{\nabla RSS_s}$
    Stochastic Gradient Descent Algorithm ()
      $\gamma_c = \frac{\kappa}{RSS_c^2}; \gamma_s = \frac{\kappa}{RSS_s^2}; \frac{\partial f}{\partial (RSS_c)} = \frac{e^{RSS_s}}{e^{RSS_c} + e^{RSS_s}}; \frac{\partial f}{\partial (RSS_s)} = \frac{e^{RSS_c}}{e^{RSS_c} + e^{RSS_s}};$
      $g_x(client) = \frac{\partial f}{\partial (RSS_c)} \cdot \nabla_x RSS_c; g_x(server) = \frac{\partial f}{\partial (RSS_s)} \cdot \nabla_x RSS_s$
      $g_y(client) = \frac{\partial f}{\partial (RSS_c)} \cdot \nabla_y RSS_c; g_y(server) = \frac{\partial f}{\partial (RSS_s)} \cdot \nabla_y RSS_s$
      $g_x = g_x(client) + g_x(server); g_y = g_y(client) + g_y(server)$
      $\vec{g} = (g_x, g_y); \|g\| = \sqrt{g_x^2 + g_y^2}$
      $\delta x = \gamma_c g_x(client) + \gamma_s g_x(server); \delta y = \gamma_c g_y(client) + \gamma_s g_y(server)$
    Relay Node Position Controller ()
      $x^{i+1} = x^i + \delta x$
      $y^{i+1} = y^i + \delta y$
    Move the relay node to position (x^{i+1}, y^{i+1})
  end while
end if

OBJECTIVE FUNCTION

A simple function that satisfies the objective of simultaneously maximizing the RSS values from both the server and client nodes would be f(pr) = RSSc(pr) + RSSs(pr); however, this results in multiple optimum positions, each resulting in a sub-optimum solution. Thus, a different objective function that satisfies all of the constraints has to be chosen. For example, Dixon and Frew [16] used f(pr) = min{SNRc(pr), SNRs(pr)} as the objective function for a similar problem statement and adopted a least squares gradient estimation (LSGE) method for determining the gradient of the objective function and to deal with the non-smooth nature of the objective function.

As our algorithm will rely purely on the spatial gradient approximation (using measurements), determining the gradients for solving a non-smooth objective function has many practical difficulties. To aid the easier integration of our proposed method, we approximate the non-smooth objective function used in to a smooth valued function by using a smoothing approximation method proposed. Furthermore, as we do not have direct SNR measurements, we use RSS measurements instead. Hence, we propose the following objective function that solves the optimization problem defined in the Equation:

$$f(p_r) = -\log(\exp(-RSS_c(p_r, p_c)) + \exp(-RSS_s(p_r, p_s))) \text{ where } p_r \in [p_{min}, p_{max}] \in \mathbb{R}^2$$

Copyright @ 2022 Author

ISSN: 2278-4632
Vol-12 Issue-01 No.01: 2022

OPTIMIZATION METHOD

The proposed function f : R → R 2 (with bounded RSS values) possesses at least one maximum value (according to the extreme value theorem). In this section, we show how this maximum value can be achieved using an appropriate optimization method. We are inclined towards gradient-based optimization methods for the advantages, such as the convergence and stability, as mentioned. Optimization methods using only an approximated gradient (of the objective function) information typically use stochastic optimization algorithms.

The gradients of the objective function are estimated using the RSS measurements and are then used to determine the future position of the relay robot, which maximizes the value of the objective function. A stochastic gradient ascent (SGA) algorithm is used to recursively update the relay node's position based on the RSS gradients as follows:

$$x_r^{i+1} = x_r^i + \gamma g_x(\vec{p}_r^{\,i})$$
$$y_r^{i+1} = y_r^i + \gamma g_y(\vec{p}_r^{\,i})$$

The relay node's position vector #»pr i = (x i r , yi r) is updated at every i−th iteration. γ ∈ R+ is the learning rate (also called "step size"), whose value will be determined in real time in each iteration. The selection of this learning rate is crucial to obtain fast convergence [38] and should satisfy the conditions P i γi = ∞ and P i γ 2 i < ∞. The choice of the learning rate γ will be discussed in Section. The multi-variate gradient vector #»g = (gx, gy) of the objective function is determined in the following way:

$$g_x = \nabla_x f = \frac{\partial f}{\partial x} = \frac{\partial f}{\partial (RSS_c)} \cdot \frac{\partial (RSS_c)}{\partial x} + \frac{\partial f}{\partial (RSS_s)} \cdot \frac{\partial (RSS_s)}{\partial x}$$
$$g_y = \nabla_y f = \frac{\partial f}{\partial y} = \frac{\partial f}{\partial (RSS_c)} \cdot \frac{\partial (RSS_c)}{\partial y} + \frac{\partial f}{\partial (RSS_s)} \cdot \frac{\partial (RSS_s)}{\partial y}$$

$$\text{where, } \frac{\partial f}{\partial (RSS_c)} = \frac{e^{RSS_s}}{e^{RSS_c} + e^{RSS_s}} \text{ and } \frac{\partial f}{\partial (RSS_s)} = \frac{e^{RSS_c}}{e^{RSS_c} + e^{RSS_s}}$$

The above method is called the stochastic gradient ascent method, because the objective function f has both deterministic and stochastic parts, as it is a function of RSS, and therefore, the stochastic gradient vector is #»g (pr) = # » ∇f(pr) + #». The #»is the noise vector in the gradient measurements at every iteration. The RSS gradient vector #»g is approximated by measurements at a single position of the relay node. Thus, we try to increase robustness and achieve fast convergence by using the concept of stochastic gradient ascent.

The SGA method requires that the objective function f(pr) is concave and the gradient g(pr) is locally Lipschitz continuous to guarantee convergence and, thus, to reach the global optimum value. We show below how the convergence requirements for the SGA method are met.

Proof for concavity: to prove that f is concave, it is necessary to show that the Hessian matrix (second-order partial derivatives) is negative semi-definite (NSD). We have the Hessian matrix,

$$H = \nabla^2(f) = \begin{bmatrix} \frac{\partial^2 f}{\partial x^2} & \frac{\partial^2 f}{\partial x \partial y} \\ \frac{\partial^2 f}{\partial y \partial x} & \frac{\partial^2 f}{\partial y^2} \end{bmatrix} = \begin{bmatrix} -\frac{\exp(RSS_c+RSS_s)}{(\exp(RSS_c)+\exp(RSS_s))^2} & \frac{\exp(RSS_c+RSS_s)}{(\exp(RSS_c)+\exp(RSS_s))^2} \\ \frac{\exp(RSS_c+RSS_s)}{(\exp(RSS_c)+\exp(RSS_s))^2} & -\frac{\exp(RSS_c+RSS_s)}{(\exp(RSS_c)+\exp(RSS_s))^2} \end{bmatrix}$$

the determinant of the Hessian matrix is zero, and both ∂ 2f ∂x2 and ∂ 2f ∂y2 are negative. This means that the Hessian matrix is NSD (as all the Eigen values are non-positive for any RSSc and RSSs value). Thus, the function f is concave.

Copyright @ 2022 Author

ISSN: 2278-4632
Vol-12 Issue-01 No.01: 2022

Proof for Lipschitz continuity: to show that the gradient function ∇f(pr) is locally Lipschitz continuous, it should be proven that there exists a positive constant L ≥ 0, such that k∇f(RSSi+1) − ∇f(RSSi)k ≤ LkRSSi+1 − RSSik in a bounded interval for RSS ∈ (RSSmin, RSSmax). Alternatively, one can prove this by showing that the derivative of ∇f (which is ∇2 f) exists and that ∇2 f is continuous and bounded in the same interval of the RSS (using the theorem, a bounded derivative implies Lipschitz continuity. We can come to this conclusion by analyzing ∇2 f in Equation and noting that in a bounded interval of the RSS (RSSmin, RSSmax) set by the threshold limits, the function ∇2 f ≤ K is bounded with a constant K depending on the RSS interval.

Stochastic optimization methods can work with noisy gradient measurements, which is a vital requirement, because the RSS measurements usually contain random variations that can be treated as a measurement noise in the optimization problem. Therefore, the key factor driving the choice of a stochastic optimization method is that the environmental factors affecting the RSS are not known prior, and hence, an optimization method that is both adaptable (to environmental changes) and robust (to noise) is needed.

Though we can reach the global optimum if f(x) is concave, the stochastic nature of the RSS is not easing this phenomenon, and hence, the objective function has multiple local optima. With careful pre-processing techniques discussed in the following subsection, the local optima issue can be mitigated. Nevertheless, as the objective is to reach the optimum in a localized region, the issue of global optimization is not a concern.

PRE-PROCESSING OF THE RSS DATA

As the measured RSS values are noisy, we propose spatial and temporal smoothing RSS filters to mitigate measurement noise and multipath fading effects.

SPATIAL SMOOTHING

It has been shown in [43] that the (spatial) multipath fading effects at each sensor can be mitigated by linear spatial averaging of the RSS measurements with several measurements per wavelength (λ) of the radio signal used. Moreover, it is mentioned that there should be a minimum spacing of 0.38λ between two RSS spacial samples to obtain independent uncorrelated measurements. Therefore, we propose to use an average filter for RSS spatial smoothing when the relay node is moving from (x i , yi) to (x i+1, yi+1). Assuming that we use the 2.4 GHz (λ = 12.5 cm) radio frequency band, the spatial sampling (note: the spatial sampling here refers to the sampling (in space) of the RSS by each sensor on the relay node, whereas the purpose of the spacing of multiple sensors within the relay node is to estimate the RSS gradient around the relay node) frequency (fs) has been set to a value greater than or equal to 5 cm, meeting both the minimum spacing for uncorrelated measurements, as well as the resolution needs of the linear spatial averaging (around 2.5 measurements per λ). The spatial averaging filer is modeled as follows:

$$RSS = \sum_{k=1}^{N} RSS(x^k, y^k), \quad \text{where } N = \frac{\left\| (x^{i+1}, y^{i+1}) - (x^i, y^i) \right\|}{f_s}$$

At each receiver, the RSS sampling time is ts = fsv, v being the velocity of the relay node. This means that the outcome of the smoothed RSS will be the RSS sample at (x i+ 1 2 , yi+ 1 2) instead of (x i+1, yi+1). As we are concerned only about the RSS gradient measurements, this spatial averaging has a positive impact.

TEMPORAL SMOOTHING

In a radio receiver, active analog filters, such as an automatic gain control (AGC) circuit, adjust the input amplification gain depending on the received signal level to protect against large signal interference and attenuate slow changes in the received signal strength caused by shadowing effects. As the objective is to mitigate fast multipath fading effects in the RSS, active analog filters are not suitable, and therefore, we propose a digital exponential moving average (EMA) filter for smoothing rapid variations in the RSS over a given time. The filter implementation is similar to a discrete first order infinite impulse response (IIR) or a single-pole low-pass filter that has a recursive feedback. The filter is characterized by the following equation:

Copyright @ 2022 Author

ISSN: 2278-4632
Vol-12 Issue-01 No.01: 2022

$$RSS^{i} = \alpha RSS^{i} + (1-\alpha)RSS^{i-1} = RSS^{i-1} + \alpha(RSS^{i} - RSS^{i-1})$$

where α is the smoothness parameter ($0 \le \alpha \le 1$) that yields the filter time constant $\tau f = \Delta T\ (\ 1-\alpha\ \alpha\ )$ and ΔT is the RSS sampling period used in the temporal smoothing. The next sub-section discusses how to determine the RSS gradients (which is a key ingredient to the SGA method) after applying spatial and temporal filters for RSS smoothing.

4. RSS THRESHOLD OPTIMIZATION AND ANALYSIS

RSS THRESHOLD OPTIMIZATION

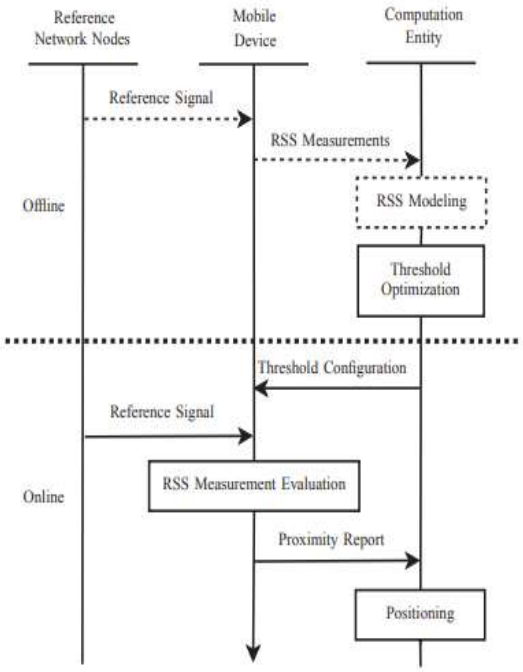

Fig. Signaling chart illustrating the proposed RSS threshold optimization procedure. The steps marked with dashed lines and in red color are optional.

we have shown how to optimize a single RSS threshold for enhanced localization performance. In what follows, we aim to validate the idea experimentally using a batch of real RSS measurements collected in an indoor bluetooth low-energy (BLE) network. The most attractive features of the BLE network as compared to other wireless networks lie in the low power consumption and efficient monitoring procedures in devices. As trade-off, more BLE beacons need to be deployed due to the shorter communication range compared to techniques based on higher transmission powers.

SENSOR DEPLOYMENT AND MEASUREMENT CAMPAIGN

We consider a typical office environment at Ericsson, Linkoping, Sweden. In total ¨ N = 10 BLE beacons are placed rather uniformly in the area. The floor plan as well as the known beacon positions are shown in two-dimensional (2-D) space in Fig, wherein a local coordinate system is used. The BLE beacons serve as transmitters and broadcast beacon information regularly. The transmit power is PT = −58 dBm. A moderate scale measurement campaign was conducted during normal work hours. Throughout the measurement campaign, the mobile device (equipped with BLE chipset) receives data packages from the BLE beacons and measures the RSS. A total number of M = 12144 RSS measurements were collected along 52 predefined tracks. During the measurement campaign, the mobile device was held approximately 1.3 meter above the ground. For clarity, we depict the 52 tracks all together in Fig. 4 and use different colors to indicate the quality of the observed RSS. Besides, Table gives the 3-D positions of the BLE beacons as well as the total number of RSS measurements collected per beacon. The obtained RSS measurements were then uploaded to the computation entity (in this case a laptop) via Wi-Fi for RSS model fitting and threshold optimization. In the above training phase, we assumed full knowledge about the position of all BLE beacons and tracks.

Copyright @ 2022 Author

ISSN: 2278-4632
Vol-12 Issue-01 No.01: 2022

Table: 3-d position of the reference network nodes (ble beacons) and the amount of rss measurements collected by each node during the offline measurement campaign.

Node ID	Position (x-,y-,z-) m	# Measurements
# 1	(2.27, 24.26, 2.60)	638 samples
# 2	(16.47, 20.34, 2.35)	1226 samples
# 3	(14.83, 11.48, 0.71)	1217 samples
# 4	(30.89, 20.36, 2.35)	1928 samples
# 5	(29.13, 14.90, 2.54)	2197 samples
# 6	(49.00, 20.34, 2.35)	203 samples
# 7	(37.74, 4.10, 2.60)	1214 samples
# 8	(18.82, 4.00, 2.60)	642 samples
# 9	(45.51, 13.30, 2.25)	1442 samples
# 10	(29.66, 4.10, 2.60)	1437 samples

FITTED RSS MODELS

We enumerated three different RSS models. In the first two linear models, we take into account the truncation effect by setting Pdec = −99 dBm. Next, we perform RSS model calibration repeatedly for each BLE beacon using the real RSS measurements. Due to space constraint, we only show some representative results. Specifically, we show the calibrated linear log-distance model, dual-mode piece-wise linear model, and nonlinear GPR model all for beacon #4 in Fig's, respectively. It is straightforward to see that the piece-wise log-distance mode can better represent the data as compared to the simplest log-distance model, but they are only able to represent the predicted mean RSS value as a simple function of the Euclidean distance between the mobile device and the reference network node. In contrast, the GPR model is able to take into account some additional information hidden in the training data about the deployment area. As was demonstrated in Fig.(a), concrete walls should have more adverse impact on the mean RSS value than glass walls.

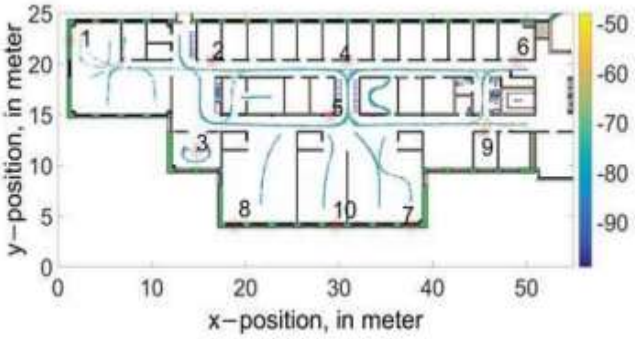

Fig. Illustration of the deployment area and the calibration set of sample positions and RSS measurements (with the strength indicated by different colors). The BLE beacons are indexed and marked by red ∗.

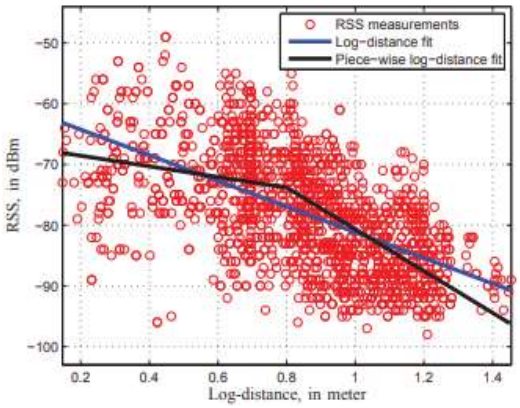

Copyright @ 2022 Author

ISSN: 2278-4632
Vol-12 Issue-01 No.01: 2022

Fig. Scatter plot of the collected RSS measurements (marked by red circles) versus the calibrated log-distance model (blue line) and piece-wise linear log distance model (black lines) for the 4th BLE beacon. The calibrated parameters for the log-distance model are Aˆ4 = −60.0145 dB, Bˆ4 = −2.1156 dB, and σˆ4 = 7.45 dB; while the calibrated parameters for the piece-wise log distance model are Aˆ1,4 = −66.81 dB, Bˆ1,4 = −0.87 dB, Bˆ2,4 = −3.50 dB, σˆ1,4 = 8.30 dB, and σˆ2,4 = 7.27 dB, and the corresponding critical distance is set to 0.8 meter (in log-scale) for this beacon.

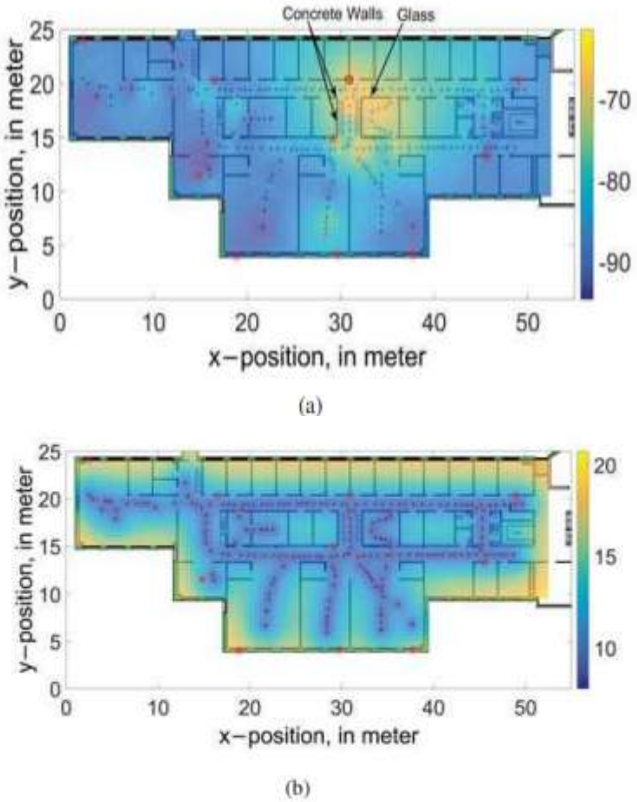

Fig. Illustration of the training data set (marked by black +) and the calibrated GPR model with parameters Aˆ4 = −69.85 dB, Bˆ4 = −1.41 dB, σˆs,4 = 3.75 dB, σˆn,4 = 2.78 dB, ˆlc,4 = 5.55 meter, for the 4th BLE beacon: (a) depicts the posterior mean and (b) depicts the posterior variance of (6).

RSS THRESHOLD OPTIMIZATION

In order to perform the RSS threshold optimization, we first generate a set X ∗ with 3038 sample positions p∗ i spread uniformly over the area, as shown in Fig.The weighting factors are set equally as w∗ i = 1/|X ∗| for all sample positions in X ∗. We note that this evaluation set X ∗ shouldn't be confused with the calibration data set used for RSS model calibration. As the localization accuracy metric, we adopt the best achievable RMSE as defined. Herein, we assume that the z-component of all sample positions is fixed to 1.3 meter and known a priori. In other words, we only concern about position estimation in x- and y-directions. As a consequence, f(p∗ i , Pth) boils down to f([x∗ i , y∗ i], Pth).

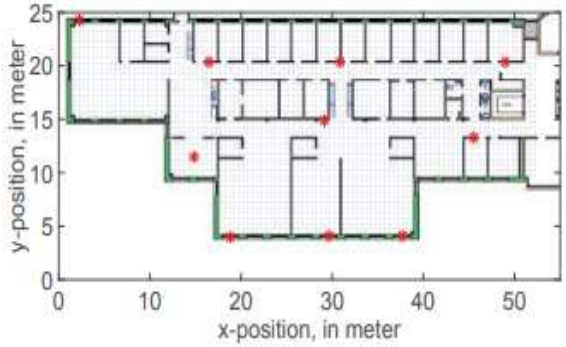

Fig. Illustration of an evaluation set of uniformly distributed sample positions (marked by blue dots), X∗.

Copyright @ 2022 Author

ISSN: 2278-4632
Vol-12 Issue-01 No.01: 2022

We repeat the steps for RSS optimization as given in Section III for the three different RSS models. In Fig, we depict the overall best achievable localization RMSE as a function of the RSS threshold Pth, which ranges from P min th = −99 dBm to P max th = −70 dBm with an increment 1 dBm. It is not surprising to have convex profiles of RMSEpos(Pth) with respect to Pth in all cases. The reason is that too large or too small threshold gives very little information about an unknown location. In order to better explain this, let us reconsider the example shown in Fig. Therein, when Popt th is set to $-\infty$ or equivalently the coverage area is infinitely large, the receiver will receive [1, 1, 1] everywhere; Similarly, when Popt th is set to $+\infty$ or equivalently the coverage area is null, the receiver will always receive [0, 0, 0]. Despite the use of different RSS models, the final RSS thresholds remain similar. In addition, we illustrate in Fig.the best achievable localization RMSE at each sample position of the evaluation set, X ∗, but only for the conventional linear log-distance RSS model and Pth = Popt th = −82 dBm. Therein, we can clearly see that the localization performance is quite good in the center of this floor, where many beacons can be received, but can be extremely bad in perimeter areas, where few beacons are received. This can be seen from Fig, where the average number of received BLE beacons reaches the maximum in the center of this floor and decreases when moving to the boundary. Appendix B gives detailed derivations for computing this quantity based on the linear log-distance RSS model. Similar results can be observed for the other two RSS models and are omitted here due to space constraint. Lastly, we note that in Fig it is obvious to see a few narrow stripe-like areas where the best achievable RMSE is relatively big. The reason is that in these areas the mobile device and the most influencing BLE beacons are nearly co-linearly located, hence the geometric dilution of precision (GDOP) or simply the geometry for positioning is extremely poor.

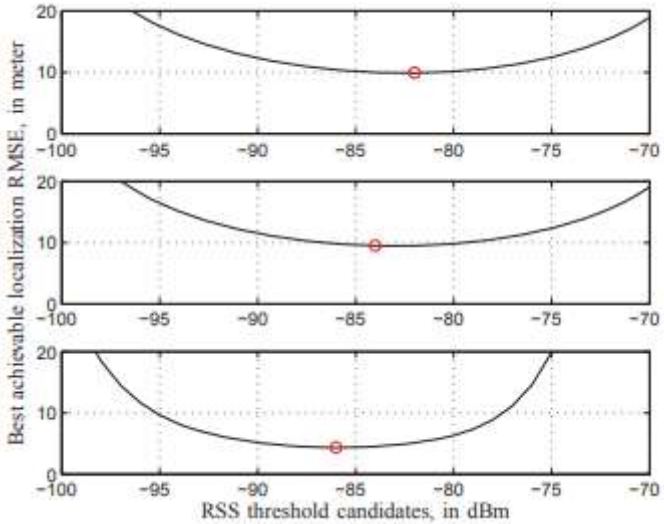

Fig. Overall best achievable localization RMSE versus threshold candidates for the linear log-distance model in subfigure-I, piece-wise linear log-distance model in subfigure-II, and Gaussian process regression model in subfigure III, respectively. The optimal RSS threshold is marked by red circle.

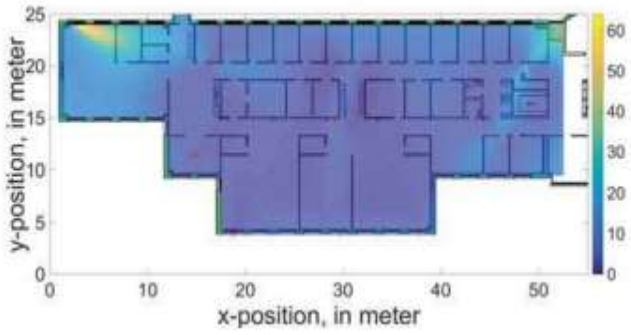

Fig. Illustration of the best achievable localization RMSE evaluated at each sample position of the evaluation set, X∗.

Copyright @ 2022 Author

ISSN: 2278-4632
Vol-12 Issue-01 No.01: 2022

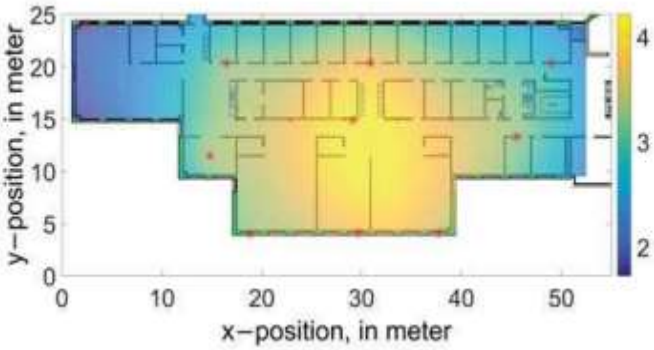

Fig. Illustration of the average number of communicating BLE beacons at each sample position of the evaluation set, X∗.

5. CONCLUSION

In this paper, we have proposed a general RSS threshold optimization procedure for indoor positioning using wireless networks. The importance of this work is to provide a fundamental baseline for converting a continuous RSS measurement to a binary proximity measurement for analyzing time series of binary proximity reports. Given the prior knowledge about the deployment information and the RSS model, a reasonable RSS threshold can be found via optimizing an adequate performance metric. As a concrete example, we have exemplified how to optimize the RSS threshold for three salient RSS models so that the best achievable localization RMSE of any unbiased position estimator is minimized. Moreover, we have conducted experimental validation of the proposed procedure in a live BLE network deployed at an office area at Ericsson. The results have shown largely enhanced localization performance when using the optimized RSS threshold, which underpins our statement that inappropriately selected RSS threshold will result in little information in the proximity measurements.

REFERENCES

- F. Yin, Y. Zhao, and F. Gunnarsson, “Proximity report triggering threshold optimization for network-based indoor positioning,” in Proc. Int. Conf. on Information Fusion, Washington D.C., USA, July 2015, pp. 1061–1069.
- “Fundamental bounds on position estimation using proximity reports,” in submitted to IEEE Int. Conf. Vehicular Technology (VTC), 2016.
- F. Gustafsson, Statistical Sensor Fusion, 2nd ed. Lund, Sweden: Studentlitteratur, 2012.
- Patwari, N.; Wilson, J. RF sensor networks for device-free localization and tracking. Proc. IEEE 2010, 98, 1961–1973.
- Kaltiokallio, O.; Bocca, M.; Patwari, N. Long-Term Device-Free Localization for Residential Monitoring. In Proceedings of the 37th Annual IEEE Conference on Local Computer Networks—Workshops, Clearwater, FL, USA, 22–25 October 2012; pp. 991–998.
- Wang, J.; Zhang, X.; Gao, Q.; Yue, H.; Wang, H.Y. Device-free Wireless Localization and Activity Recognition: A Deep Learning Approach. IEEE Trans. Veh. Technol. 2017, 66, 6258–6267.
- M. Hazas and J. Ward, ―A novel broadband ultrasonic location system,‖ Proc. 4th Int. Conf. Ubiquitous Computing, pp. 264-280, 2002.
- R. Want, A. Hopper, V. Falcao and J. Gibbons, ―The active badge location system,‖ ACM Transactions on Information Systems, vol. 10, no 1, pp. 91-102, 1992.
- G. Giorgetti, S. K. S. Gupta, and G. Manes, “Optimal RSS threshold selection in connectivity-based localization schemes,” in Proc. Int. Symp. on Modeling, Analysis and Simulation of Wireless and Mobile Systems. New York, NY, USA: ACM, 2008, pp. 220–228.
- Y. Zhao, F. Yin, and F. Gunnarsson, “Particle filtering for positioning based on proximity reports,” in Proc. Int. Conf. on Information Fusion, Washington, D.C., USA, July 2015.
- Wen-Feng, L. I. , and F. U. Xiu-Wen . "Survey on Invulnerability of Wireless Sensor Networks." Chinese Journal of Computers 38(2015).
- Mahapatro, A , and P. Khilar . "Fault Diagnosis in Wireless Sensor Networks: A Survey." IEEE Access 15.4(2013):2000-2026.

Copyright @ 2022 Author